Title
Selective vulnerabilities in the proteostasis network of castration-resistant prostate cancer

Journal
Cell Chemical Biology, 29(3)

ISSN
2451-9456

Authors
Shkedi, Arielle
Taylor, Isabelle R
Echtenkamp, Frank
et al.

Publication Date
2022-03-01

DOI
10.1016/j.chembiol.2022.01.008

Peer reviewed

HHS Public Access

Author manuscript

Cell Chem Biol. Author manuscript; available in PMC 2023 March 17.

Published in final edited form as:

Cell Chem Biol. 2022 March 17; 29(3): 490–501.e4. doi:10.1016/j.chembiol.2022.01.008.

Selective Vulnerabilities in the Proteostasis Network of Castration-Resistant Prostate Cancer (CRPC)

Arielle Shkedi[1,⊥], **Isabelle R. Taylor**[1,⊥], **Frank Echtenkamp**[3], **Poornima Ramkumar**[2], **Mohamed Alshalalfa**[4], **Génesis M. Rivera-Márquez**[3], **Michael A. Moses**[3], **Hao Shao**[1], **R. Jeffrey Karnes**[5], **Len Neckers**[3], **Felix Feng**[4], **Martin Kampmann**[2], **Jason E. Gestwicki**[1,*]

[1]Department of Pharmaceutical Chemistry and the Institute for Neurodegenerative Disease, University of California San Francisco, San Francisco, CA 94158

[2]Department of Biochemistry and Biophysics and the Institute for Neurodegenerative Disease, University of California San Francisco, San Francisco, CA 94158

[3]Urologic Oncology Branch, Center for Cancer Research, National Cancer Institute, Bethesda, MD 20892

[4]Radiation Oncology, Helen Diller Comprehensive Cancer Center, University of California, San Francisco

[5]Department of Urology, Mayo Clinic, Rochester, MN 55902

SUMMARY

Castration-resistant prostate cancer (CRPC) is associated with an increased reliance on protein homeostasis (aka proteostasis) factors, such as heat shock protein 70 (Hsp70), but it is not clear what other factors might be involved. To address this question, we perform functional and synthetic lethal screens in four prostate cancer cell lines. These screens confirm key roles for Hsp70, Hsp90 and their co-chaperones, but also suggest that the mitochondrial chaperone, Hsp60/HSPD1 is selectively required in CRPC cell lines. Knockdown of Hsp60 does not impact the stability of androgen receptor (AR) or its variants; rather, it is associated with loss of mitochondrial spare respiratory capacity, partly due to increased proton leakage. Finally, transcriptional data reveals a correlation between Hsp60 levels and poor survival of prostate cancer patients. These findings suggest that re-wiring of the proteostasis network is associated with CRPC, creating selective vulnerabilities that might be targeted to treat the disease.

[*] Lead Contact, Jason E. Gestwicki, Tel: 1 415 502 7121, Jason.gestwicki@ucsf.edu.

[⊥]these authors contributed equally

Author Contributions

A.S., I.R.T., F.E., P.R., M.A., G.M.R.-V., M.A.M. and H.S. designed and conducted experiments and interpreted results. R.J.K., L.N., F.F., M.K., and J.E.G. interpreted results and provided resources. A.S., I.R.T. and J.E.G. prepared the manuscript, with assistance from the other authors.

Disclosures

J.E.G. holds patents to the use of Hsp70 inhibitors and is a member of the Cell Chemical Biology Scientific Advisory Board. The authors declare no other competing interests.

eTOC blurb

Drug targets for castration-resistant prostate cancer (CRPC) are needed. The protein homeostasis (proteostasis) pathways are known to include targets; however a systematic search had not been performed. Here, Shkedi and Taylor *et al.* use an shRNA screen targeting ~130 proteostasis factors to identify Hsp60 as a selective vulnerability in CRPC.

Graphical Abstract

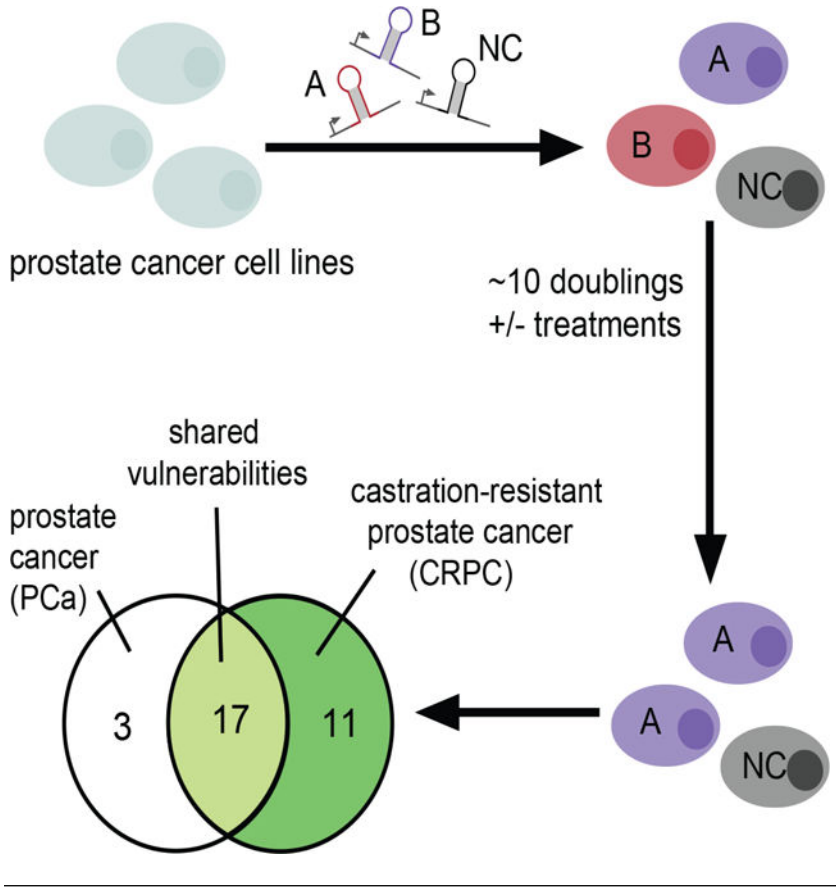

INTRODUCTION

Protein homeostasis (proteostasis) is achieved when the overall rates of protein folding, trafficking, and degradation are balanced (Balch et al., 2008). This balance is maintained by the proteostasis network, a collection of interconnected pathways, which include molecular chaperones, stress response signaling factors and protein quality control systems. In cancer cells, unique demands are placed on the proteostasis network, owing to their rapid growth rates, unusual metabolic requirements, and high mutational loads (Brodsky and Chiosis, 2006; Chaudhury et al., 2006; Powers et al., 2009; Whitesell and Lindquist, 2005). This dependence has been described as a “non-oncogene addiction” (Luo et al., 2009; Nagel et al., 2016) and individual components of the proteostasis network have been pursued as attractive anti-cancer targets. In the clinic, such attempts have yielded both dramatic successes and confounding failures (Crawford et al., 2011). One potential reason for this

uneven level of success is that the field is only beginning to probe how proteostasis networks are functionally different in cancer cells vs. normal cells or between different stages of cancer (Calderwood and Gong, 2016; Gabai et al., 2016; Rodina et al., 2016; Wu et al., 2020).

Prostate cancer (PCa) is an especially interesting system for probing these questions. PCa cells typically rely on transcriptional programs driven by the androgen receptor (AR), and many prostate tumors therefore initially respond well to androgen deprivation therapy (ADT). However, following ADT, the disease invariably progresses to castration-resistant prostate cancer (CRPC) (Heinlein and Chang, 2004; Kirby et al., 2011; Logothetis et al., 2013). In CRPC cells, AR activity is usually able to persist through amplification, mutations, constituitively-active splice variants of AR (ARv) (Antonarakis et al., 2014; Grasso et al., 2012; Montgomery et al., 2008; Quigley et al., 2018; Watson et al., 2015) and compensation by other steroid hormone receptors (SHRs), such as the glucocorticoid receptor (Arora et al., 2013; Puhr et al., 2018). Additionally, the conversion from PCa to CRPC is associated with metabolic reprogramming (Massie et al., 2011). Thus, it seems likely that, to account for these molecular and metabolic changes, the proteostasis networks of PCa and CRPC cells might need to be distinct. For example, like other SHRs, AR is known to require an elaborate set of chaperones, including heat shock protein 70 (Hsp70), heat shock protein 90 (Hsp90) and their co-chaperones, for its folding, activation and degradation (Echeverria and Picard, 2010; Kirschke et al., 2014; Pratt et al., 2006; Pratt and Toft, 2003). Accordingly, chemical inhibitors of Hsp90 are known to promote degradation of AR in PCa cells (Moses et al., 2018) and these inhibitors show synergy with ADT (Chen et al., 2016). Similar findings have been observed when targeting essential Hsp90 co-chaperones (De Leon et al., 2011). However, Hsp90 inhibitors are less effective in cellular models of CRPC, such as 22Rv1, which are partly driven by ARv signaling. Instead, inhibitors of Hsp70 have been shown to decrease the stability of ARvs and have anti-proliferative activity in these cells (Moses et al., 2018). This difference in chaperone inhibitor sensitivity between PCa and CRPC cells might be partially explained by differences in molecular recognition of AR and its variants. Specifically, Hsp70, but not Hsp90, binds to the N-terminal motif that remains in the ARv found in 22Rv1 cells (Dong et al., 2019; Eftekharzadeh et al., 2019). Thus, CRPC is an interesting model for studying the role of proteostasis networks, given the reliance of these cells on Hsp70, Hsp90, AR and its variants.

While there is growing evidence for the roles of Hsp70 and Hsp90 in PCa and CRPC, it is not yet clear whether the broader proteostasis network might be “re-wired” to accommodate the demands of CRPC. Here, we used functional genomics screening to identify selective vulnerabilities in PCa and CRPC cell lines. In that effort, we deployed a focused shRNA collection, termed the Proteostasis Library (Abrams et al., 2021), that allows knockdown of ~140 molecular chaperones, co-chaperones, chaperonins and related factors. In addition, we searched for synthetic lethality by repeating the screens in the presence of chemical inhibitors of Hsp70 and Hsp90. Together, the results identified factors that are required in all of the cells (*e.g.* shared vulnerabilities), but also ones that are unique to PCa or CRPC cell lines. One of the most striking findings was that the mitochondrial chaperonin, Hsp60 (gene name HSPD1) is required for growth of CRPC cells, but not PCa cells. Knockdown studies suggest that, unlike Hsp70 and Hsp90, this chaperonin is not involved in AR or

ARv stability; rather, decreases in Hsp60 levels in 22Rv1 cells were associated with loss of mitochondrial spare respiratory capacity. The importance of the relationship between Hsp60 and CRPC was further validated by analysis of transcriptional data from prostate cancer patient samples, which showed a strong correlation between Hsp60 transcript levels and poor disease outcomes. Together, these results identify a potential drug target for the treatment of CRPC, as well as more broadly suggest how proteostasis networks might be adapted to provide drug resistance in prostate cancer.

RESULTS

Design of the Proteostasis Library

To explore the chaperone dependences of PCa and CRPC cell lines, we used a focused shRNA library, termed the Proteostasis Library, that targets 139 genes encoding chaperones and related factors (Figure 1A; see below). This library is composed of 25 targeting sequences per gene (listed in Supplemental Table 1), plus an additional 500 control, non-targeting sequences. These shRNA sequences are cloned into a lentiviral vector and used in a pooled screen format, as previously described (Abrams et al., 2021; Kampmann et al., 2013; Kampmann et al., 2015). The genes selected for inclusion in this library include examples of the major chaperone families, such as Hsp70s, Hsp90s, chaperonins (TRiC/CCT and Hsp60/HSPD1) and small heat shock proteins (sHsps) (Figure 1A). It also includes the major co-chaperones for Hsp70s, such as J-domain proteins (JDPs, also called Hsp40s), tetratricopeptide repeat (TPR) domain proteins and nucleotide-exchange factors (NEFs), and the major co-chaperones for Hsp90, such as CDC37, AHA1 and PTGES3 (also called p23). Beyond chaperones, chaperonins and co-chaperones, the library includes other protein folding and maintenance enzymes, such as protein disulfide isomerases (PDIs), peptidyl prolyl isomerases (PPIases), and factors required for proteasome assembly (*e.g.* PSMG1) and protein trafficking (*e.g.* VCP/97, Sec63). Finally, the library covers a subset of targets that are involved in stress signaling pathways, including HSF1/2, ATF6 and XBP1. It is worth noting that, although CRISPR/Cas9-based methods are also a powerful, alternative way to perform screens, we favored the shRNA approach in this particular case because it can be used in multiple cell lines without the requirement for stable expression of Cas9/dCas9. Together, this shRNA library provides broad coverage of the major functional and regulatory components of the proteostasis network, allowing potential identification of cancer sensitivities across various functions.

In assembling the Proteostasis Library, we favored groups of targets that are known to physically bind to each other (bold and dotted lines in Figure 1A). One of the defining features of the proteostasis network is that many of the components engage in protein-protein interactions (PPIs), both with each other and with their client proteins (Freilich et al., 2018). Another feature of this network is that there is potential redundancy built into it. For example, in human cells there are genes for ~13 Hsp70s, ~50 JDPs, and 6 Hsp90s (Chen et al., 2005; Kampinga et al., 2009; Radons, 2016). To illustrate this feature in Figure 1A, we clustered the genes in functional families and depict them as a schematic map that highlights the PPIs. For each class, there are members that are localized to specific sub-cellular locations; for example, the major Hsp70s of the cytosol are Hsp72 (HSPA1A) and Hsc70

(HSPA8), while BiP/HSPA5 and mortalin/HSPA9 are found in the ER and mitochondria, respectively (Rosenzweig et al., 2019).

Functional genomics screen to identify shared and unique vulnerabilities in PCa and CRPC cell lines

Using the Proteostasis Library, we conducted a functional genomics screen by transducing cells with the pooled shRNAs, growing them for 10 doubling times, and then deep sequencing at the initial (T_0) and final (T_{final}) time points (Figure 1B). Results on the individual shRNA level showed that the screens produced viable results and the negative controls behaved as expected (Supplemental Figure 1). From these results, we determined the phenotype and p-value of each gene knockdown (Supplemental Table 2), as described (Kampmann et al., 2013). Here, phenotype is calculated by comparing the shRNA frequencies at the T_0 and T_{final} time points, along with the cell growth rate, and the Mann-Whitney P-value is calculated by comparing the results of the 25 shRNAs per gene to the negative control shRNAs.

These screens were conducted in four different cell lines. Two of these lines (22Rv1 and C4–2) are androgen-insensitive CRPC cells. The 22Rv1 cells express both full-length AR and the truncated form (ARv7), whereas the C4–2 cells express only full-length AR. As controls, we performed the screens in two additional PCa cell lines: an AR positive, androgen-sensitive cell line (LNCaP), and an AR-negative cell line (PC3) (Figure 1C). For each of the four cell lines, the screens identified proteostasis factors important for growth (Figure 2A). These factors are highlighted in Figure 2A, but also labelled in bold in Supplemental Table 2. One of the first observations was that only a small subset of proteostasis factors (~10%) were identified as “hits” in any of the cell lines. This limited sensitivity was most dramatic for the PC3 cell line, where only 4/139 (3%) genes were considered “hits” (P-value < 0.01; Figure 2A). This finding suggests that PC3 cells, and to a lesser extent the other cell lines, can tolerate partial loss of many/most proteostasis factors; however, because this is a pooled screen, it also remains likely that there are false negatives. Regardless, the low percentage of “hits” allowed us to rapidly focus on the most sensitive factors.

To explore the similarities and differences between the cell lines in more detail, we established a cut-off of P-value < 0.01 ($-\log_{10}$(P-value) > 2) and then combined the vulnerabilities from the CRPC (22Rv1 and C4–2) cell lines and compared them to the LNCaP cell lines. At this point, the PC3 data were excluded due to the low hit rate. This comparative analysis identified 17 “hits” that are largely shared across the cell lines (*e.g.* shared vulnerabilities), as well as 3 unique vulnerabilities for the LNCaP cells and 11 hits unique to CRPC (Figure 2B). The shared vulnerabilities included a subset of Hsp70s and Hsp40/JDPs, as well as TriC/CCT, Hsp10 (gene name HSPE1) and VCP/p97 (Figure 2B, heat map). This result was satisfying because, as mentioned above, Hsp70s, Hsp90s, and JDPs, have a well-characterized role in AR processing (Echeverria and Picard, 2010; Kirschke et al., 2014; Pratt et al., 2006). Interestingly, these AR processing factors were not identified in the PC3 cell line, which does not express AR or ARv, but were shared in the LNCaP, 22Rv1 and C4–2 cell lines which do (see Fig 1C). It seems likely that

some of the other shared factors are involved in general cancer cell growth and survival, and indeed, VCP/p97, has been previously identified as being broadly important in prostate cancer (Tsujimoto et al., 2004).

Next, to better visualize the selective vulnerabilities, we plotted the $-\log_{10}P$ for each gene in the LNCaP experiments vs. each of the two CRPC cell lines (Figure 2C). We also plotted the sensitivities onto the shRNA library maps to look for physical/functional relationships (Supplemental Figure 2). Through this analysis, we observed that the LNCaP cells appear to have a reliance on HSPA4 (an Hsp70 isoform) and PTGES3 (p23), the latter of which has been associated with both Hsp90-dependent and independent roles in transcription (Echtenkamp et al., 2011; Freeman et al., 2000). Next, we turned our attention to the factors that were identified as selective vulnerabilities in the CRPC cells. Most strikingly, this analysis showed that 22Rv1 and C4–2 cells depend on the mitochondrial chaperonin, Hsp60/HSPD1. Hsp60 is known to form a complex in the mitochondria with Hsp10/HSPE1, which is a shared hit among all 4 tested cell lines. The C4–2 cells also relied on GRPEL1, another mitochondria-localized chaperone that is thought to be involved in mitochondrial protein folding and import. Together, these results suggested that CRPC cells have selective vulnerabilities in the proteostasis network and that a number of these cluster to the mitochondrial sub-network.

Synthetic lethality screens with Hsp70 and Hsp90 inhibitors highlight Hsp60 as an important selective vulnerability in CRPC cells

Because Hsp70 and Hsp90 are known to be involved in AR processing, we wondered whether repeating the shRNA screens in the presence of chemical inhibitors of these chaperones might reveal synthetic lethalities. First, we characterized the effects of these inhibitors on AR and ARv in our hands. Consistent with the literature (Moses et al., 2018), we found that treatment with AUY-922 (an inhibitor of Hsp90; Figure 3A) leads to loss of full length (FL) AR in 22Rv1, LNCaP, and C4–2 after 6 hours (Figure 3B). We also confirmed that AUY-922 was unable to affect the variant AR (ARv) in 22Rv1 cells. On the other hand, treatment with JG-231 (an inhibitor of Hsp70) only mildly reduced FL AR, but was effective in reducing ARv in the 22Rv1 cells (Figure 3B).

Guided by these results, we repeated the shRNA screen in the 22Rv1, C4–2 and LNCaP cell lines in the presence of JG-231 or AUY-922. Cells were treated three times throughout the growth period with either JG-231 or AUY-922, at established concentrations that were found to have anti-proliferative effects while still allowing cells to recover and continue growing (see Methods). Through the calculations described earlier, we determined the phenotype and P-value of genetic knockdown in each of these conditions. We found that the main “hits” from these chemical-genetic screens could be binned into 3 categories – shared, cell-line specific, and drug-treatment specific (Figure 3C). Among the shared and cell-line specific hits, we found that the vulnerabilities were largely similar between the initial screen and the chemical-genetic screen. For example, Hsp70 isoforms (gene name HSPA8, HSPA9, HSPA14), the JDPs (DNAJA3, DNAJC8), and the TRiC complex (CCT4, CCT7, CCT8) remain essential in the presence of either inhibitor (Figure 3C). Consistent with this idea, hierarchical clustering revealed overall, similar patterns of genetic vulnerabilities

(Supplemental Figure 3). However, novel hits emerged as well. For example, we found that the cytosolic Hsp90 gene (HSP90AB1) was essential in the presence of the Hsp90 inhibitor (AUY-922) in all three cell lines. Moreover, HSP90AB1 was also essential in 22Rv1 cells after Hsp70 inhibition. These strong interactions suggested, perhaps not surprisingly, that the proteostasis network becomes more reliant on Hsp90s when this chaperone is partially inhibited. Interestingly, the co-chaperone HOP/STIP1, which is known to bind both Hsp70 and Hsp90 (Bhattacharya et al., 2020; Johnson et al., 1998), was also only required in the presence of AUY-922. This result suggests that the communication between these chaperones might become more important upon Hsp90 inhibition. Another striking finding from this synthetic lethal screen was that Hsp60/HSPD1 was again found to be a strong vulnerability only in the 22Rv1 and C4–2 cells, but not the LNCaP (Figure 3C). Overall, these results validated our previous observations and suggested that Hsp60 could be an interesting target in CRPC cells.

Hsp60 is a selective vulnerability in CRPC cells

Hsp60 is a mitochondrial chaperonin, homologous to the bacterial GroEL, which is involved in mitochondrial protein folding (Bukau and Horwich, 1998; Pace et al., 2013). To validate the Hsp60 result from the screen, we transduced 22Rv1, C4–2, LNCaP and PC3 cells with 2 different RFP-labeled shRNAs or a scrambled negative control, and selected with puromycin. In 22Rv1 cells, knockdown was >90% for both shRNA sequences, but not the control (Figure 4A). The cells were then maintained for 3 weeks and the percentage of RFP-positive cells was monitored during every passage by flow cytometry (Supplemental Figure 4). From these studies, we observed depletion of the RFP-positive population in the 22Rv1 (Figure 4B) and C4–2 cells, but not LNCaP or PC3 cells (Figure 4C). To understand whether this reliance on Hsp60 was restricted to CRPC cell lines, we knocked it down in multiple other cancer subtypes, with a focus on breast cancer (MCF7 and MDA-MD-231) and multiple myeloma (KMS-11, KMS-34, OPM-2, AMO-1) cell lines because of their established connections with chaperones and proteostasis (Sannino and Brodsky, 2017; Sha and Goldberg, 2020). We found that 4/6 cell lines did not rely on Hsp60/HSPD1 for growth (Figure 4C and Supplemental Figure 4). In 2/6 cell lines (MCF-7 and KMS-34), only a partial decrease (about 50% depletion compared to the control) in the RFP population was observed. Thus, the CRPC cell lines had an unusual, but not entirely exclusive, reliance on Hsp60/HSPD1.

Hsp60 knockdown does not affect AR levels

While Hsp70 and Hsp90 directly regulate AR stability (see Fig 3B), we considered it unlikely that Hsp60 would operate through a similar mechanism due to it’s mitochondrial localization. However, the expression of AR and ARv is known to be sensitive to manipulation of metabolic pathways, such as inhibition of fatty acid metabolism (Schlaepfer et al., 2014; Zadra et al., 2019), so it seemed possible that Hsp60 could regulate AR stability through indirect mechanisms. Thus, we examined whether Hsp60 knockdown reduced AR levels in the dox-inducible 22Rv1 cells. These cells were treated with dox for 96 hours, which produced a robust knockdown of Hsp60 without any impact on AR or ARv (Figure 5A). These results suggest that Hsp60 is involved in survival of CRPC cells through a mechanism that is independent of AR stability.

Metabolic effects of Hsp60 KD

Another possibility is that Hsp60 could be important for metabolic reprogramming in CRPC cell lines. To test this idea, we monitored the impact of Hsp60 loss on mitochondrial respiration in 22Rv1 cells using the Mito Stress Test (Agilent). In this assay, oligomycin, trifluoromethoxy carbonylcyanide phenylhydrazone (FCCP), and Rotenone/Antimycin A are sequentially added to cultured cells to calculate mitochondrial activity and capacity (Figure 5B). Upon 5-day treatment with dox, Hsp60-knockdown suppressed numerous aspects of mitochondrial respiration. In general, Hsp60 loss resulted in lower basal oxygen consumption; however, this effect was relatively minor compared to the decrease in the maximal oxygen consumption rate (OCR; Figure 5C). Loss of Hsp60 consistently reduced the spare respiratory capacity (maximal OCR – basal OCR) of 22Rv1 cells and was generally accompanied by an increase in proton leakage, an indication that the integrity of the electron transport chain (ETC) and/or the inner membrane are disrupted (Figures 5E and 5F). These effects were often accompanied by variable impacts on basal respiration and glycolytic response, indicating that Hsp60 is more important in maintaining mitochondrial plasticity than it is in maintaining basal respiration in 22Rv1 cells (Figure 5D). These effects were reproducible with an alternative shRNA sequence and similar results were observed in independent replicates (Supplemental Figure 5).

Clinical significance of Hsp60 in CRPC

Lastly, we wanted to examine if Hsp60 expression had a clinical correlation to patient outcomes in prostate cancer, and especially in those individuals who had been previously treated with ADT. Towards that goal, we analyzed metastasis-free survival in ADT-treated (n=243) and non-ADT treated (n=476) patients from the Decipher GRID database, which were pooled from two matched cohorts previously (Karnes et al., 2018), and compared them based on Hsp60/HSPD1 gene transcript levels. Here, high Hsp60 expression was defined as greater than the median of all patients. Strikingly, ADT-treated patients with high Hsp60 expression had significantly worse outcomes (Figure 6, HR=1.95, $p = 0.00024$). In the patients who had not received ADT (no-ADT), those with high Hsp60 expression have slightly worse metastasis-free survival outcomes (HR=1.4), but this finding was not statistically significant ($p = 0.02$). These findings suggest that high Hsp60 levels correlate with worse metastasis-free survival in prostate cancer patients, especially in those patients previously treated with ADT. This result is consistent with the idea that Hsp60 is especially important in CRPC cells.

DISCUSSION

Given the established dependence of prostate cancer cells on AR signaling, the proteostasis network has been suggested to contain putative drug targets (Ballar Kirmizibayrak et al., 2020). Here, we used focused shRNA screens to search for additional proteostasis factors that might be required for cell growth and survival in CRPC and PCa cell lines. Through these studies, we discovered “hits” that are shared amongst all the cell lines, such as the TriC/CCT complex, VCP/p97, and Hsp10. Both TriC/CCT and VCP/p97 have been broadly implicated in tumorigenesis (Anderson et al., 2015; Boudiaf-Benmammar et al., 2013), so this shared dependence was consistent with probable roles in sustaining general cancer

phenotypes, such as rapid growth and proliferation. Here, we were more interested in those factors that were selective for growth of CRPC cell lines. Among the findings, we became most interested in Hsp60/HSPD1, which was only identified as a strong hit in the CRPC cell lines (22Rv1 and C4–2). This chaperonin had previously been linked to clinical prostate cancer (Beyene et al., 2018; Castilla et al., 2010), so this finding seemed most promising.

Hsp60 is known to be involved in mitochondrial protein folding and translocation (Bukau and Horwich, 1998; Cheng et al., 1989; Pace et al., 2013). It has been shown to have various roles in cancer, such as glioblastoma (Polson et al., 2018; Tang et al., 2016) and non-small cell lung cancer (NSCLC) (Parma et al., 2021), but its exact function has not been determined. Proteomics studies have identified a number of substrates of Hsp60, including malate dehydrogenase and other TCA cycle-related proteins (Bie et al., 2020). We found that knockdown of Hsp60/HSPD1 does not affect AR levels, but rather has a strong effect on mitochondrial spare respiratory capacity (see Figure 5D). Spare respiratory capacity is a strong predictor of metastatic potential, given that it is related to a cell's ability to respond to diverse stress stimuli (Marchetti et al., 2020). As cancer cells escape their tissue of origin, they encounter environments that differ substantially from the nutritional characteristics to which they are accustomed. Spare respiratory capacity likely plays an important role in supporting foreign cells' ability to thrive in such envionments thereby promoting prostate cancer ability to escape it's natural environment and thrive in foreign nutrient environments. Our results support a model in which prostate cancer becomes increasingly reliant on Hsp60 as it deviates from androgen-dependent growth and escapes the prostate. By promoting the activity of components of the ETC, Hsp60 helps CRPC cells resist the stress related to metastatic growth. In general support of this idea, Hsp60 has recently been found to regulate oxidative phosphorylation in NSCLC cells, through effects on cytochrome c oxidase and the creatine transporter SLC6A8 (Parma et al., 2021). In addition, knockdown of Hsp60 has recently been shown to activate autophagy in adipose tissue (Hauffe et al., 2021) and treatment with an Hsp60 inhibitor induces autophagy in glioblastoma cells (Polson et al., 2018). This autophagy induction could be a compensatory response to delay apoptosis. This relationship between Hsp60, metabolism and cell survival appears to be important in patients, as we observed in clinical data that low Hsp60 expression significantly correlates with metastasis-free survival in prostate tumors from patients treated with ADT. Morever, Hsp60 is upregulated after 8 weeks in a mouse model of CRPC development (Akamatsu et al., 2015). These findings generally agree with our *in vitro* observations that Hsp60 plays a special role in CRPC cell lines, but not LNCaP or PC3. Hsp60 (and its prokaryotic ortholog, GroEL) has been the target of multiple drug discovery and chemical biology campaigns (Chapman et al., 2009; Polson et al., 2018; Shao et al., 2020; Stevens et al., 2020; Wiechmann et al., 2017). The present study suggests that CRPC might be a promising disease target for these emerging inhibitors.

More broadly, it seems likely that the proteostasis networks of prostate cancer cells are re-programmed during disease progression and the onset of ADT resistance. Thus, whether an inhibitor of proteostasis works for a specific prostate cancer stage might depend on multiple factors, including the prior treatment regime. Functional genetic tools such as the Proteostasis Library, plus other biochemical technologies (Rizzolo et al., 2017; Rodina et al.,

2016; Taipale et al., 2014), may begin to unravel these selective vulnerabilities for prostate cancer and other indications.

STAR METHODS

Resource Availability

Lead contact—Further information and requests for resources and reagents should be directed to and will be fulfilled by the Lead Contact, Jason E. Gestwicki (Jason.gestwicki@ucsf.edu).

Materials availability—Correspondence and requests for materials should be addressed to the Lead Contact.

Data and code availability—All data are available in the main text or as Supplemental information. The full list of sequences for the shRNA library are in Supplemental Table 1 and the full list of p-values are in Supplemental Table 2. This paper includes an analysis of existing, publically available data; for more information see (Karnes et al., 2018). All other data is available from the corresponding author upon request. This paper does not report original code. Any additional information required to reanalyze the data reported in this paper is available from the lead contact upon request

Experimental Model and Subject Details

Cell lines—PC3, LNCaP, C4–2, and 22Rv1 cells were purchased from ATCC and grown in RPMI 1640 medium (Sigma R7388) supplemented with 10% non heat-inactivated fetal bovine serum (Gibco 16000044) and 1% penicillin/streptomycin (Millipore-Sigma, 11074440001). HEK293T cells (ATCC) were cultured in Dulbecco's Modified Eagle Medium (DMEM; Gibco 12430112) supplemented with 10% non heat-inactivated fetal bovine serum (Gibco 16000044) and 1% penicillin/streptomycin. All cell lines were maintained in regular tissue culture-treated flasks (Greiner C7106), with the exception of the low-adherent LNCaPs, which were kept in carboxyl-coated flasks (Corning 354778). All cells were grown at 37 °C and 5% CO_2.

Lentiviral production and transduction—All lentiviruses were prepared by transfection into HEK293T cells using Lipofectamine 2000 and packaging plasmids pMol, pRSV, and pVSV-g. Viral particles were allowed to form for 48 hours post transfection, and then the viral supernatant was collected, passed through a 0.45 μm filter, and stored at 4 °C for no longer than one week prior to use. Viral supernatant was added to suspended cells immediately following trypsinization, along with 8 μg/mL polybrene (Santa Cruz sc-134220). The cells were allowed to adhere to the flasks, then the medium was replaced with regular growth medium after 6–8 hours. After 48 hours, the cells successfully infected with the lentiviral plasmids were selected with 1 μg/mL puromycin (Gibco A11138–03) for an additional 48 hours. Flow cytometry was used to determine infection and selection efficiency via the expression of fluorescent markers encoded by the lentiviral vectors (generally BFP for pooled shRNA screens, and mCherry or TurboRFP for individual shRNA constructs).

Method Details

Reagents—JG-231 was prepared in house, as described (Shao et al., 2018). AUY-922 was purchased from Advanced ChemBlocks Inc. (cat # 10274). The Proteostasis shRNA Library was prepared as previously described (Abrams et al., 2021). Briefly, sequences were cloned into the lentiviral backbone plasmid, pMK1275. For verification, individual shRNAs were cloned into either the dox-inducible backbone, pMK1201 (derived from pINDUCER10 of the Elledge Lab) or pMK1200.

Pooled shRNA screens and individual shRNA validation—Lentivirus was prepared as described above of the pooled shRNA library and used to infect the prostate cancer cell lines. Most cell lines were initially infected at ~50–60% efficiency, monitored by BFP intensity, and then were further selected with puromycin to ~100%. Immediately following the selection T_0 samples, of ~4 million cells each, were collected and stored at −80 °C until genomic DNA was isolated for sequencing. The cells were continually cultured, maintaining at least 4 million cells with each passage, for a period of ~10 doublings. For screens with chaperone inhibitors, the cells were dosed three times at the concentrations listed in Table 1, for a duration of 24 hours each time. Concentrations were chosen by determining the IC_{50} per cell line by MTT assay, then further optimized by testing multiple concentrations at around the IC_{50} and observing the effects on cells after treatment and multiple days of recovery. Final concentrations were chosen as ones that induced cell death for a sizable population, but still allowed the cells to recover and continue growing, to reduce potential bottlenecking. At the end of the growth period, samples of ~4 million cells were collected for the T_{final} sample. For individual shRNA validation, lentivirus was prepared as described, cells were transduced and monitored by RFP intensity. Cells were then further selected with puromycin, so the final population was 50–80% RFP-positive. The percentage of RFP positive cells was then monitored by flow cytometry over a ~2 week period, with cells being split at a 1:4 ratio whenever confluency was reached.

	Screen conditions	Screen conditions
Cell Line	JG-231 (μM)	AUY-922 (nM)
22Rv1	0.75	100
PC3	0.5	100
LNCaP	1	100
C4-2	1	100

Genomic DNA isolation, indexing and PCR purification—Genomic DNA was extracted using MN NucleoSpin® Blood Kit (Macherey-Nagel 740951) for ~4–6 million cells per sample. Whole genomic DNA samples were carried forward into indexing PCRs using Q5® High-Fidelity polymerase (New England BioLabs M0492S). PCR amplified, and indexed, fragments of approximately 280 bp were purified by a two-step SPRI bead purification (43), and concentrations were determined on a Qubit Fluorometer before pooling for deep sequencing on a HiSeq 4000.

Mito stress test—Stable 22Rv1 cells containing dox inducible-expressing shRNA constructs (shRNA-Hsp60–1 or Hsp60–2) were stimulated with 100 ng/mL doxycycline for 4 days prior to seeding 2.0×10^4 cells/well in a 96 well plate. Oxygen consumption (OCR) and extracellular acidification rate (ECAR) were monitored with Agilent SeaHorse XFe96 ~18h after seeding with XF DMEM pH 7.4 containing glucose, pyruvate, and glutamine. All experiments were normalized by DNA quantification with Cyquant (ThermoFisher) and are the result of at least 4 replicates per condition. Spare respiratory capacity (maximal OCR – basal OCR) and proton leakage (oligomycin-sensitive OCR – non-mitochondrial OCR) were calculated using Wave (Agilent).

Data analysis and clustering—Genes were clustered hierarchically by P-value in Cluster (Eisen et al., 1998) and displayed by Java TreeView (Saldanha, 2004).

Immunoblotting—Cells were grown in a 6-well plate to near 100% confluency, after which the medium was replaced with fresh medium containing the compounds in 1% DMSO. The compound was left on the cells and incubated at 37 °C and 5% CO_2 for six hours, immediately followed by harvesting and lysing in M-PER supplemented with protease inhibitors. Lysate concentrations were quantified by a bicinchoninic acid assay (BCA, ThermoFisher 23227) and then run on 4–15% gradient SDS polyacrylamide gels at 5–10 μg of total protein per sample. All blot quantification was performed in Image Lab™ software (BioRad). The antibodies used are found in the Key Resource Table. Dilutions are as follows: Anti-AR (1:1000), Anti-Hsc70/p70 (1:200), Anti-Hsp27 (1:200), Anti-Hsp60 (1:1000), Anti-Hsp10 (1:1000), Anti-actin (1:200).

Clinical data analysis—Expression profiles of retrospective radical prostatectomy samples from 719 patients (243 with ADT treatment, 476 no treatment) were retrieved from the Decipher GRID database. Patient cohorts were pooled from two matched cohorts previously (Karnes et al., 2018). Patients were grouped based on expression of Hsp60/HSPD1. High Hsp60 was defined as higher than median expression. The additional clinical characteristics of two arms are shown in Supplemental Table 3.

Quantification and Statistical Analysis—Unless otherwise specified, data plotting and statistical analyses were performed using Prism 7 (GraphPad Software). Statistical significance was evaluated by one-way ANOVA with independent post-hoc Tukey's multiple comparison test and was defined as a p-value of less than 0.05. To compare two groups, Student's t-test and two-way ANOVA were used. Details on the number of technical and biological (independent) replicates of each experiment can be found in the figure legends. In Kaplan-Meier analysis (Figure 6), the log-rank test was used to evaluate the differences in survival amongst the Hsp60 high/low groups.

Supplementary Material

Refer to Web version on PubMed Central for supplementary material.

Acknowledgements

This work was supported by grants from StandUp2Cancer (J.E.G. and M.K.), the US Department of Defense PC150065 Idea Development Award (J.E.G. and L.N.), NIH/NCI CA181494 (M.K.), the Stephen and Nancy Grand Multiple Myeloma Translational Initiative (M.K.). L.N., F.E., M.A.M., G.M.R.-V. were supported with funds from the Intramural Program, Center for Cancer Research, National Cancer Institute, to L.N. under Investigator Initiated Project Number ZIA SC 010074.

Citations

Abrams J, Arhar T, Mok SA, Taylor IR, Kampmann M, and Gestwicki JE (2021). Functional genomics screen identifies proteostasis targets that modulate prion protein (PrP) stability. Cell Stress Chaperones 26, 443–452. [PubMed: 33547632]

Akamatsu S, Wyatt AW, Lin D, Lysakowski S, Zhang F, Kim S, Tse C, Wang K, Mo F, Haegert A, et al. (2015). The Placental Gene PEG10 Promotes Progression of Neuroendocrine Prostate Cancer. Cell reports 12, 922–936. [PubMed: 26235627]

Anderson DJ, Le Moigne R, Djakovic S, Kumar B, Rice J, Wong S, Wang J, Yao B, Valle E, Kiss von Soly S, et al. (2015). Targeting the AAA ATPase p97 as an Approach to Treat Cancer through Disruption of Protein Homeostasis. Cancer cell 28, 653–665. [PubMed: 26555175]

Antonarakis ES, Lu C, Wang H, Luber B, Nakazawa M, Roeser JC, Chen Y, Mohammad TA, Chen Y, Fedor HL, et al. (2014). AR-V7 and resistance to enzalutamide and abiraterone in prostate cancer. N Engl J Med 371, 1028–1038. [PubMed: 25184630]

Arora VK, Schenkein E, Murali R, Subudhi SK, Wongvipat J, Balbas MD, Shah N, Cai L, Efstathiou E, Logothetis C, et al. (2013). Glucocorticoid receptor confers resistance to antiandrogens by bypassing androgen receptor blockade. Cell 155, 1309–1322. [PubMed: 24315100]

Balch WE, Morimoto RI, Dillin A, and Kelly JW (2008). Adapting proteostasis for disease intervention. Science 319, 916–919. [PubMed: 18276881]

Ballar Kirmizibayrak P, Erbaykent-Tepedelen B, Gozen O, and Erzurumlu Y (2020). Divergent Modulation of Proteostasis in Prostate Cancer. Adv Exp Med Biol 1233, 117–151. [PubMed: 32274755]

Beyene DA, Naab TJ, Kanarek NF, Apprey V, Esnakula A, Khan FA, Blackman MR, Brown CA, and Hudson TS (2018). Differential expression of Annexin 2, SPINK1, and Hsp60 predict progression of prostate cancer through bifurcated WHO Gleason score categories in African American men. The Prostate 78, 801–811. [PubMed: 29682763]

Bhattacharya K, Weidenauer L, Luengo TM, Pieters EC, Echeverria PC, Bernasconi L, Wider D, Sadian Y, Koopman MB, Villemin M, et al. (2020). The Hsp70-Hsp90 co-chaperone Hop/Stip1 shifts the proteostatic balance from folding towards degradation. Nature communications 11, 5975.

Bie AS, Comert C, Korner R, Corydon TJ, Palmfeldt J, Hipp MS, Hartl FU, and Bross P (2020). An inventory of interactors of the human HSP60/HSP10 chaperonin in the mitochondrial matrix space. Cell Stress Chaperones 25, 407–416. [PubMed: 32060690]

Boudiaf-Benmammar C, Cresteil T, and Melki R (2013). The cytosolic chaperonin CCT/TRiC and cancer cell proliferation. PLoS One 8, e60895. [PubMed: 23613750]

Brodsky JL, and Chiosis G (2006). Hsp70 molecular chaperones: emerging roles in human disease and identification of small molecule modulators. Curr Top Med Chem 6, 1215–1225. [PubMed: 16842158]

Bukau B, and Horwich AL (1998). The Hsp70 and Hsp60 chaperone machines. Cell 92, 351–366. [PubMed: 9476895]

Calderwood SK, and Gong J (2016). Heat Shock Proteins Promote Cancer: It's a Protection Racket. Trends Biochem Sci.

Castilla C, Congregado B, Conde JM, Medina R, Torrubia FJ, Japon MA, and Saez C (2010). Immunohistochemical expression of Hsp60 correlates with tumor progression and hormone resistance in prostate cancer. Urology 76, 1017 e1011–1016.

Chapman E, Farr GW, Furtak K, and Horwich AL (2009). A small molecule inhibitor selective for a variant ATP-binding site of the chaperonin GroEL. Bioorg Med Chem Lett 19, 811–813. [PubMed: 19110421]

Chaudhury S, Welch TR, and Blagg BS (2006). Hsp90 as a Target for Drug Development. ChemMedChem.

Chen B, Piel WH, Gui L, Bruford E, and Monteiro A (2005). The HSP90 family of genes in the human genome: Insights into their divergence and evolution. Genomics 86, 627–637. [PubMed: 16269234]

Chen L, Li J, Farah E, Sarkar S, Ahmad N, Gupta S, Larner J, and Liu X (2016). Cotargeting HSP90 and Its Client Proteins for Treatment of Prostate Cancer. Mol Cancer Ther 15, 2107–2118. [PubMed: 27390342]

Cheng MY, Hartl FU, Martin J, Pollock RA, Kalousek F, Neupert W, Hallberg EM, Hallberg RL, and Horwich AL (1989). Mitochondrial heat-shock protein hsp60 is essential for assembly of proteins imported into yeast mitochondria. Nature 337, 620–625. [PubMed: 2645524]

Crawford LJ, Walker B, and Irvine AE (2011). Proteasome inhibitors in cancer therapy. Journal of cell communication and signaling 5, 101–110. [PubMed: 21484190]

De Leon JT, Iwai A, Feau C, Garcia Y, Balsiger HA, Storer CL, Suro RM, Garza KM, Lee S, Kim YS, et al. (2011). Targeting the regulation of androgen receptor signaling by the heat shock protein 90 cochaperone FKBP52 in prostate cancer cells. Proc Natl Acad Sci U S A 108, 11878–11883. [PubMed: 21730179]

Dong J, Wu Z, Wang D, Pascal LE, Nelson JB, Wipf P, and Wang Z (2019). Hsp70 Binds to the Androgen Receptor N-terminal Domain and Modulates the Receptor Function in Prostate Cancer Cells. Mol Cancer Ther 18, 39–50. [PubMed: 30297360]

Echeverria PC, and Picard D (2010). Molecular chaperones, essential partners of steroid hormone receptors for activity and mobility. Biochim Biophys Acta 1803, 641–649. [PubMed: 20006655]

Echtenkamp FJ, Zelin E, Oxelmark E, Woo JI, Andrews BJ, Garabedian M, and Freeman BC (2011). Global functional map of the p23 molecular chaperone reveals an extensive cellular network. Mol Cell 43, 229–241. [PubMed: 21777812]

Eftekharzadeh B, Banduseela VC, Chiesa G, Martinez-Cristobal P, Rauch JN, Nath SR, Schwarz DMC, Shao H, Marin-Argany M, Di Sanza C, et al. (2019). Hsp70 and Hsp40 inhibit an inter-domain interaction necessary for transcriptional activity in the androgen receptor. Nature communications 10, 3562.

Eisen MB, Spellman PT, Brown PO, and Botstein D (1998). Cluster analysis and display of genome-wide expression patterns. Proc Natl Acad Sci U S A 95, 14863–14868. [PubMed: 9843981]

Freeman BC, Felts SJ, Toft DO, and Yamamoto KR (2000). The p23 molecular chaperones act at a late step in intracellular receptor action to differentially affect ligand efficacies. Genes Dev 14, 422–434. [PubMed: 10691735]

Freilich R, Arhar T, Abrams JL, and Gestwicki JE (2018). Protein-Protein Interactions in the Molecular Chaperone Network. Acc Chem Res 51, 940–949. [PubMed: 29613769]

Gabai VL, Yaglom JA, Wang Y, Meng L, Shao H, Kim G, Colvin T, Gestwicki J, and Sherman MY (2016). Anticancer Effects of Targeting Hsp70 in Tumor Stromal Cells. Cancer Res 76, 5926–5932. [PubMed: 27503927]

Grasso CS, Wu YM, Robinson DR, Cao X, Dhanasekaran SM, Khan AP, Quist MJ, Jing X, Lonigro RJ, Brenner JC, et al. (2012). The mutational landscape of lethal castration-resistant prostate cancer. Nature 487, 239–243. [PubMed: 22722839]

Hauffe R, Rath M, Schell M, Ritter K, Kappert K, Deubel S, Ott C, Jahnert M, Jonas W, Schurmann A, et al. (2021). HSP60 reduction protects against diet-induced obesity by modulating energy metabolism in adipose tissue. Mol Metab 53, 101276. [PubMed: 34153520]

Heinlein CA, and Chang C (2004). Androgen receptor in prostate cancer. Endocr Rev 25, 276–308. [PubMed: 15082523]

Johnson BD, Schumacher RJ, Ross ED, and Toft DO (1998). Hop modulates Hsp70/Hsp90 interactions in protein folding. J Biol Chem 273, 3679–3686. [PubMed: 9452498]

Kampinga HH, Hageman J, Vos MJ, Kubota H, Tanguay RM, Bruford EA, Cheetham ME, Chen B, and Hightower LE (2009). Guidelines for the nomenclature of the human heat shock proteins. Cell Stress Chaperones 14, 105–111. [PubMed: 18663603]

Kampmann M, Bassik MC, and Weissman JS (2013). Integrated platform for genome-wide screening and construction of high-density genetic interaction maps in mammalian cells. Proc Natl Acad Sci U S A 110, E2317–2326. [PubMed: 23739767]

Kampmann M, Horlbeck MA, Chen Y, Tsai JC, Bassik MC, Gilbert LA, Villalta JE, Kwon SC, Chang H, Kim VN, et al. (2015). Next-generation libraries for robust RNA interference-based genome-wide screens. Proc Natl Acad Sci U S A 112, E3384–3391. [PubMed: 26080438]

Karnes RJ, Sharma V, Choeurng V, Ashab HA, Erho N, Alshalalfa M, Trock B, Ross A, Yousefi K, Tsai H, et al. (2018). Development and Validation of a Prostate Cancer Genomic Signature that Predicts Early ADT Treatment Response Following Radical Prostatectomy. Clin Cancer Res 24, 3908–3916. [PubMed: 29760221]

Kirby M, Hirst C, and Crawford ED (2011). Characterising the castration-resistant prostate cancer population: a systematic review. Int J Clin Pract 65, 1180–1192. [PubMed: 21995694]

Kirschke E, Goswami D, Southworth D, Griffin PR, and Agard DA (2014). Glucocorticoid receptor function regulated by coordinated action of the Hsp90 and Hsp70 chaperone cycles. Cell 157, 1685–1697. [PubMed: 24949977]

Logothetis CJ, Gallick GE, Maity SN, Kim J, Aparicio A, Efstathiou E, and Lin SH (2013). Molecular classification of prostate cancer progression: foundation for marker-driven treatment of prostate cancer. Cancer Discov 3, 849–861. [PubMed: 23811619]

Luo J, Solimini NL, and Elledge SJ (2009). Principles of cancer therapy: oncogene and non-oncogene addiction. Cell 136, 823–837. [PubMed: 19269363]

Marchetti P, Fovez Q, Germain N, Khamari R, and Kluza J (2020). Mitochondrial spare respiratory capacity: Mechanisms, regulation, and significance in non-transformed and cancer cells. FASEB J 34, 13106–13124. [PubMed: 32808332]

Massie CE, Lynch A, Ramos-Montoya A, Boren J, Stark R, Fazli L, Warren A, Scott H, Madhu B, Sharma N, et al. (2011). The androgen receptor fuels prostate cancer by regulating central metabolism and biosynthesis. EMBO J 30, 2719–2733. [PubMed: 21602788]

Montgomery RB, Mostaghel EA, Vessella R, Hess DL, Kalhorn TF, Higano CS, True LD, and Nelson PS (2008). Maintenance of intratumoral androgens in metastatic prostate cancer: a mechanism for castration-resistant tumor growth. Cancer Res 68, 4447–4454. [PubMed: 18519708]

Moses MA, Kim YS, Rivera-Marquez GM, Oshima N, Watson MJ, Beebe K, Wells C, Lee S, Zuehlke AD, Shao H, et al. (2018). Targeting the Hsp40/Hsp70 chaperone axis as a novel strategy to treat castration-resistant prostate cancer. Cancer Res.

Nagel R, Semenova EA, and Berns A (2016). Drugging the addict: non-oncogene addiction as a target for cancer therapy. EMBO Rep 17, 1516–1531. [PubMed: 27702988]

Pace A, Barone G, Lauria A, Martorana A, Piccionello AP, Pierro P, Terenzi A, Almerico AM, Buscemi S, Campanella C, et al. (2013). Hsp60, a novel target for antitumor therapy: structure-function features and prospective drugs design. Curr Pharm Des 19, 2757–2764. [PubMed: 23092316]

Parma B, Ramesh V, Naidu Gollavilli P, Siddiqui A, Pinna L, Schwab A, Marshall S, Zhang S, Pilarsky C, Napoli F, et al. (2021). Metabolic impairment of non-small cell lung cancers by mitochondrial HSPD1 targeting. J Exp Clin Cancer Res 40, 248–268.

Polson ES, Kuchler VB, Abbosh C, Ross EM, Mathew RK, Beard HA, da Silva B, Holding AN, Ballereau S, Chuntharpursat-Bon E, et al. (2018). KHS101 disrupts energy metabolism in human glioblastoma cells and reduces tumor growth in mice. Science translational medicine 10.

Powers MV, Clarke PA, and Workman P (2009). Death by chaperone: HSP90, HSP70 or both? Cell Cycle 8, 518–526. [PubMed: 19197160]

Pratt WB, Morishima Y, Murphy M, and Harrell M (2006). Chaperoning of glucocorticoid receptors. Handb Exp Pharmacol, 111–138. [PubMed: 16610357]

Pratt WB, and Toft DO (2003). Regulation of signaling protein function and trafficking by the hsp90/hsp70-based chaperone machinery. Exp Biol Med (Maywood) 228, 111–133. [PubMed: 12563018]

Puhr M, Hoefer J, Eigentler A, Ploner C, Handle F, Schaefer G, Kroon J, Leo A, Heidegger I, Eder I, et al. (2018). The Glucocorticoid Receptor Is a Key Player for Prostate Cancer Cell Survival and a Target for Improved Antiandrogen Therapy. Clin Cancer Res 24, 927–938. [PubMed: 29158269]

Quigley DA, Dang HX, Zhao SG, Lloyd P, Aggarwal R, Alumkal JJ, Foye A, Kothari V, Perry MD, Bailey AM, et al. (2018). Genomic Hallmarks and Structural Variation in Metastatic Prostate Cancer. Cell 175, 889. [PubMed: 30340047]

Radons J (2016). The human HSP70 family of chaperones: where do we stand? Cell Stress Chaperones 21, 379–404. [PubMed: 26865365]

Rizzolo K, Huen J, Kumar A, Phanse S, Vlasblom J, Kakihara Y, Zeineddine HA, Minic Z, Snider J, Wang W, et al. (2017). Features of the Chaperone Cellular Network Revealed through Systematic Interaction Mapping. Cell reports 20, 2735–2748. [PubMed: 28903051]

Rodina A, Wang T, Yan P, Gomes ED, Dunphy MP, Pillarsetty N, Koren J, Gerecitano JF, Taldone T, Zong H, et al. (2016). The epichaperome is an integrated chaperome network that facilitates tumour survival. Nature 538, 397–401. [PubMed: 27706135]

Rosenzweig R, Nillegoda NB, Mayer MP, and Bukau B (2019). The Hsp70 chaperone network. Nature Reviews Molecular Cell Biology 20, 665–680. [PubMed: 31253954]

Saldanha AJ (2004). Java Treeview--extensible visualization of microarray data. Bioinformatics 20, 3246–3248. [PubMed: 15180930]

Sannino S, and Brodsky JL (2017). Targeting protein quality control pathways in breast cancer. BMC Biol 15, 109. [PubMed: 29145850]

Schlaepfer IR, Rider L, Rodrigues LU, Gijon MA, Pac CT, Romero L, Cimic A, Sirintrapun SJ, Glode LM, Eckel RH, et al. (2014). Lipid catabolism via CPT1 as a therapeutic target for prostate cancer. Mol Cancer Ther 13, 2361–2371. [PubMed: 25122071]

Sha Z, and Goldberg AL (2020). Multiple myeloma cells are exceptionally sensitive to heat shock, which overwhelms their proteostasis network and induces apoptosis. Proc Natl Acad Sci U S A 117, 21588–21597. [PubMed: 32817432]

Shao H, Li X, Moses MA, Gilbert LA, Kalyanaraman C, Young ZT, Chernova M, Journey SN, Weissman JS, Hann B, et al. (2018). Exploration of Benzothiazole-Rhodacyanines as Allosteric Inhibitors of Protein-Protein Interactions with Heat Shock Protein 70 (Hsp70). J Med Chem.

Shao H, Oltion K, Wu T, and Gestwicki JE (2020). Differential scanning fluorimetry (DSF) screen to identify inhibitors of Hsp60 protein-protein interactions. Org Biomol Chem 18, 4157–4163. [PubMed: 32458889]

Stevens M, Howe C, Ray AM, Washburn A, Chitre S, Sivinski J, Park Y, Hoang QQ, Chapman E, and Johnson SM (2020). Analogs of nitrofuran antibiotics are potent GroEL/ES inhibitor pro-drugs. Bioorg Med Chem 28, 115710. [PubMed: 33007545]

Taipale M, Tucker G, Peng J, Krykbaeva I, Lin ZY, Larsen B, Choi H, Berger B, Gingras AC, and Lindquist S (2014). A quantitative chaperone interaction network reveals the architecture of cellular protein homeostasis pathways. Cell 158, 434–448. [PubMed: 25036637]

Tang H, Li J, Liu X, Wang G, Luo M, and Deng H (2016). Down-regulation of HSP60 Suppresses the Proliferation of Glioblastoma Cells via the ROS/AMPK/mTOR Pathway. Scientific reports 6, 28388. [PubMed: 27325206]

Tsujimoto Y, Tomita Y, Hoshida Y, Kono T, Oka T, Yamamoto S, Nonomura N, Okuyama A, and Aozasa K (2004). Elevated expression of valosin-containing protein (p97) is associated with poor prognosis of prostate cancer. Clin Cancer Res 10, 3007–3012. [PubMed: 15131036]

Watson PA, Arora VK, and Sawyers CL (2015). Emerging mechanisms of resistance to androgen receptor inhibitors in prostate cancer. Nature reviews 15, 701–711.

Whitesell L, and Lindquist SL (2005). HSP90 and the chaperoning of cancer. Nature reviews 5, 761–772.

Wiechmann K, Muller H, Konig S, Wielsch N, Svatos A, Jauch J, and Werz O (2017). Mitochondrial Chaperonin HSP60 Is the Apoptosis-Related Target for Myrtucommulone. Cell chemical biology 24, 614–623 e616. [PubMed: 28457707]

Wu PK, Hong SK, Chen W, Becker AE, Gundry RL, Lin CW, Shao H, Gestwicki JE, and Park JI (2020). Mortalin (HSPA9) facilitates BRAF-mutant tumor cell survival by suppressing ANT3-mediated mitochondrial membrane permeability. Science signaling 13.

Zadra G, Ribeiro CF, Chetta P, Ho Y, Cacciatore S, Gao X, Syamala S, Bango C, Photopoulos C, Huang Y, et al. (2019). Inhibition of de novo lipogenesis targets androgen receptor signaling in castration-resistant prostate cancer. Proc Natl Acad Sci U S A 116, 631–640. [PubMed: 30578319]

Highlights

- Prostate cancer cells depend on proteostasis pathways for survival.
- Functional genomics screens reveal that CRPC cells depend on Hsp60.
- Hsp60 is required for a CRPC-related metabolic switch, not AR stability.
- Hsp60 is a promising drug target for CRPC.

SIGNIFICANCE

Prostate cancer (PCa) is amongst the most common cancers in men. While treatments for early stages of this disease are effective, there is an urgent need for better treatments in the advanced stages, such as castration-resistant prostate cancer (CRPC). The molecular chaperones, such as Hsp70 and Hsp90, have been closely linked to PCa and CRPC, because of their ability to stabilize the androgen receptor (AR) and its variants. Here, we used a functional genomics approach to reveal whether other chaperones might also be important for survival of CRPC cells. Specifically, we performed screens in four PCa and CRPC cell lines, using shRNA libraries targeting ~140 chaperones, chaperonins, co-chaperones and related proteins. We also repeated the screens using chemical inhibitors of Hsp70 and Hsp90 to reveal potential synthetic lethality relationships. The results suggest that Hsp60 is a promising drug target for CRPC, a finding that is supported by evidence for high Hsp60 transcript levels in patients. These results are significant because they provide support for a potential treatment strategy. More broadly, the work illustrates a way to identify selective vulnerabilities and synthetic lethal relationships in cancer and other diseases, using focused shRNA libraries in combination with chemical inhibitors of key proteostasis nodes.

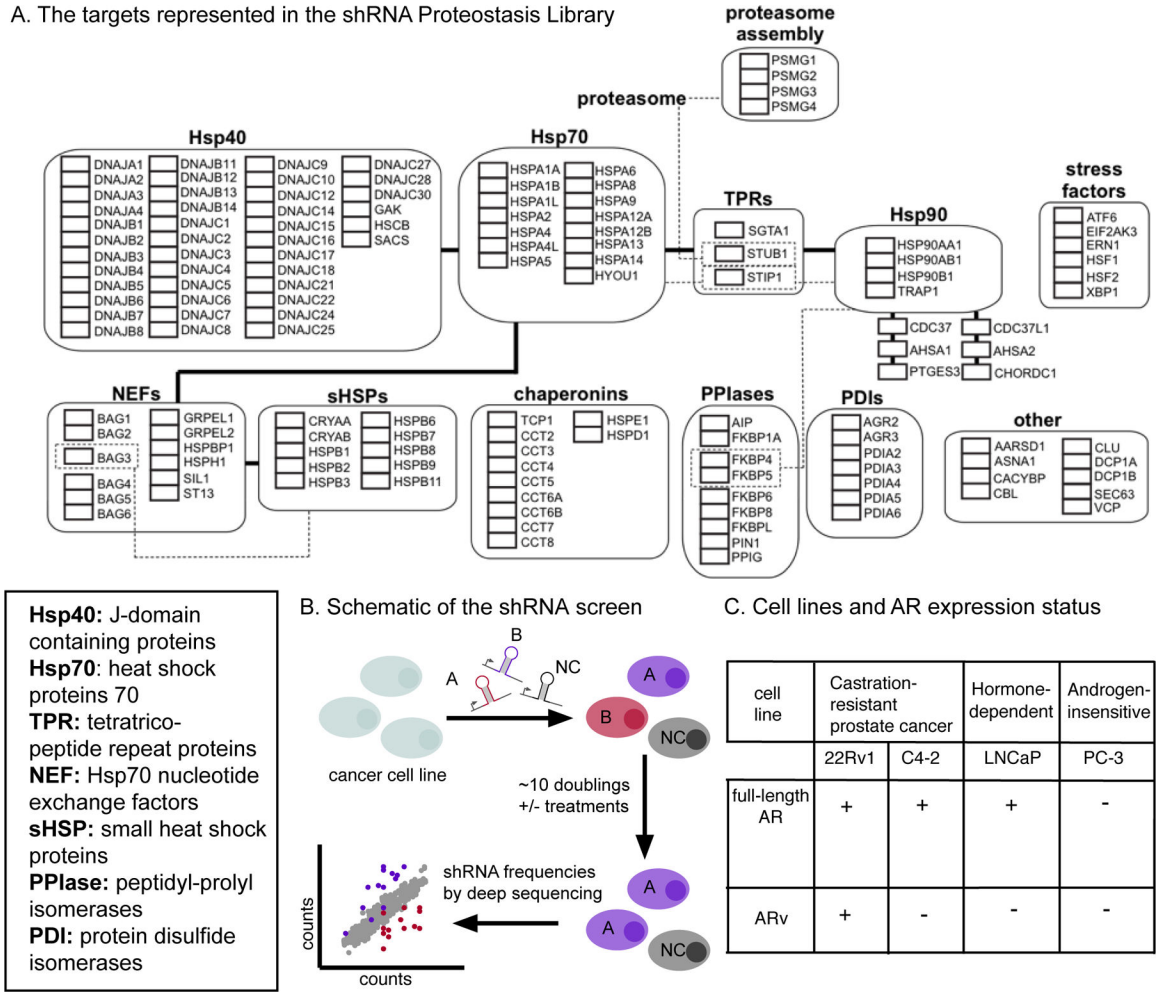

Figure 1.

Functional genomic screen in PCa cell lines. A. Map of the chaperones and other proteostasis targets represented in the shRNA Proteostasis Library. Targets are grouped by structural categories (e.g. Hsp70s, sHSPs). The bold lines between the categories represent known physical connections (e.g. protein-protein interactions). The dotted lines represent connections that are specific to only the indicated members of the class. B. Schematic of the workflow for the functional genomics screen. Cells are transduced with lentivirus expressing targeting (A, B, etc.) and ~500 non-targeting negative control (NC) sequences. After selections performed with or without proteostasis stressors, the enrichment or depletion of specific shRNA sequences is quantified by deep sequencing and comparison of T_0 to T_{final}. C. Four prostate cancer cell lines, organized by hormone sensitivity and AR expression status.

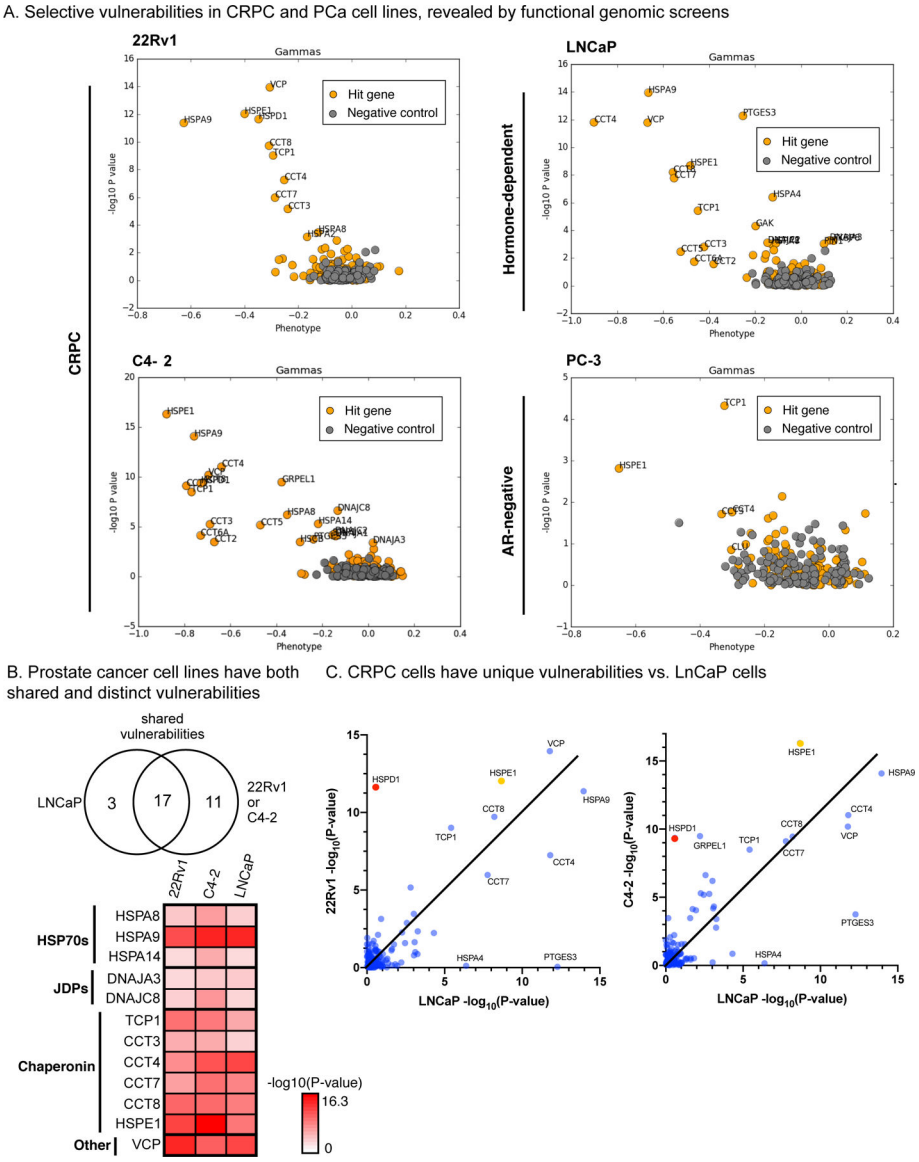

Figure 2.

CRPC cell lines have unique vulnerabilities that are distinct from PCa cells. A. Volcano plots, showing the results of the functional genomics screen for each of the four cell lines. B. Comparisons between the CRPC cell lines (22Rv1 and C4–2) and the PCa cell lines (LNCaP) reveals both shared and distinct subsets of vulnerabilities. All genes with −log10(P-value) >2 in all 3 cell lines are shown. C. To illustrate differences between the LNCaP and CRPC cell lines, the −log10(P-value) are plotted against each other, such that those genes far from the diagonal are preferentially required in one cell line and not the other. For reference, HSPD1 is shown in red and HSPE1 in orange.

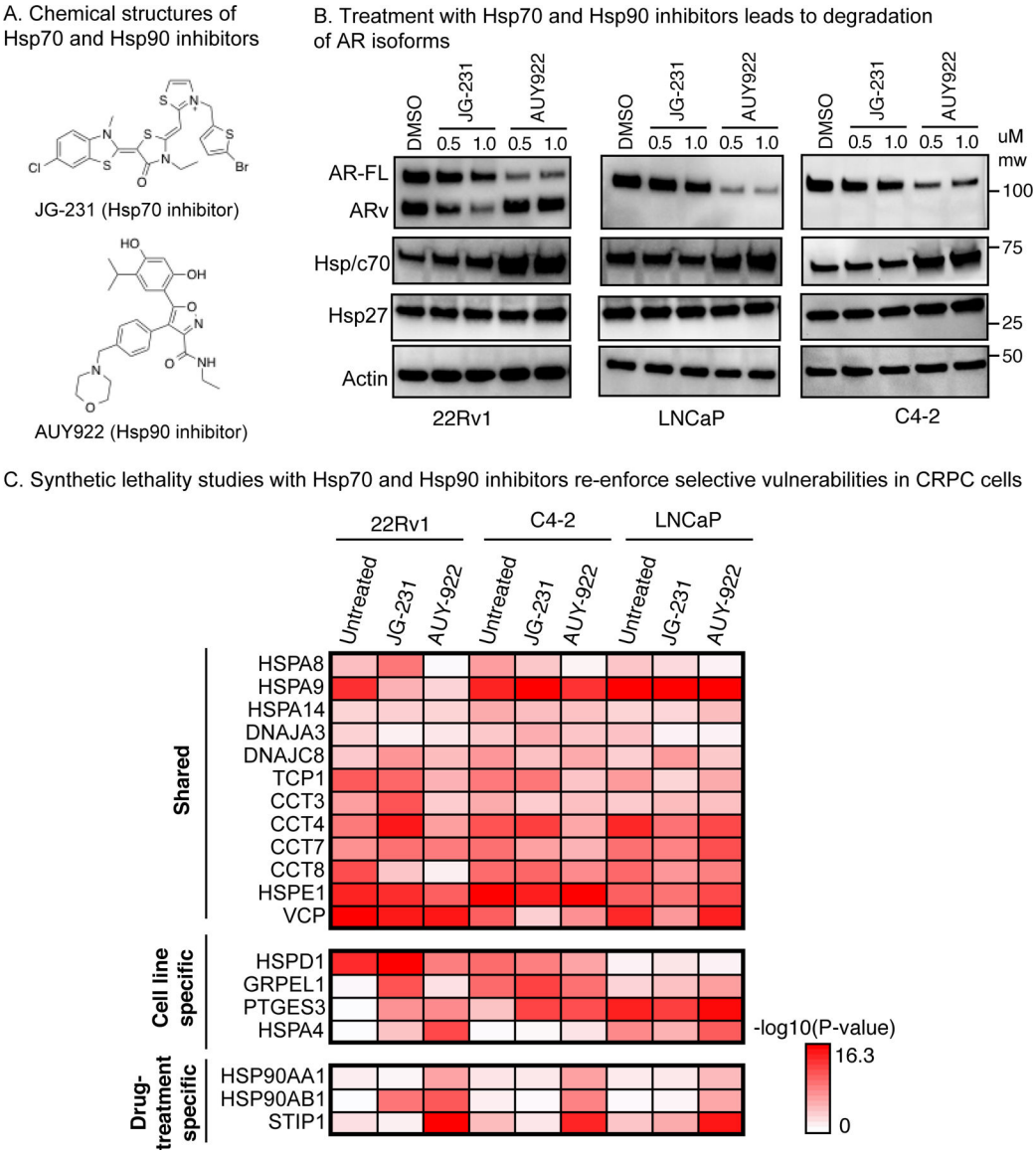

Figure 3.

Synthetic lethality studies, using chemical inhibitors of Hsp70 and Hsp90, suggest that CRPC cells depend on Hsp60/HSPD1. A. Chemical structure of the compounds used in this study. JG-231 and AUY-922 are pan-inhibitors of Hsp70 and Hsp90, respectively. B. Treatment with AUY-922 leads to degradation of full-length AR and treatment with JG-231 leads to degradation of ARv in prostate cancer cell lines. Experiments are representative of studies performed in triplicate. C. P-values of selected genes show various patterns of knockdown sensitivity across prostate cancer cells. Shared and cell line specific “hits” from the untreated condition generally remain hits with Hsp70 and Hsp90 inhibition, and some drug-treatment specific sensitivites are revealed.

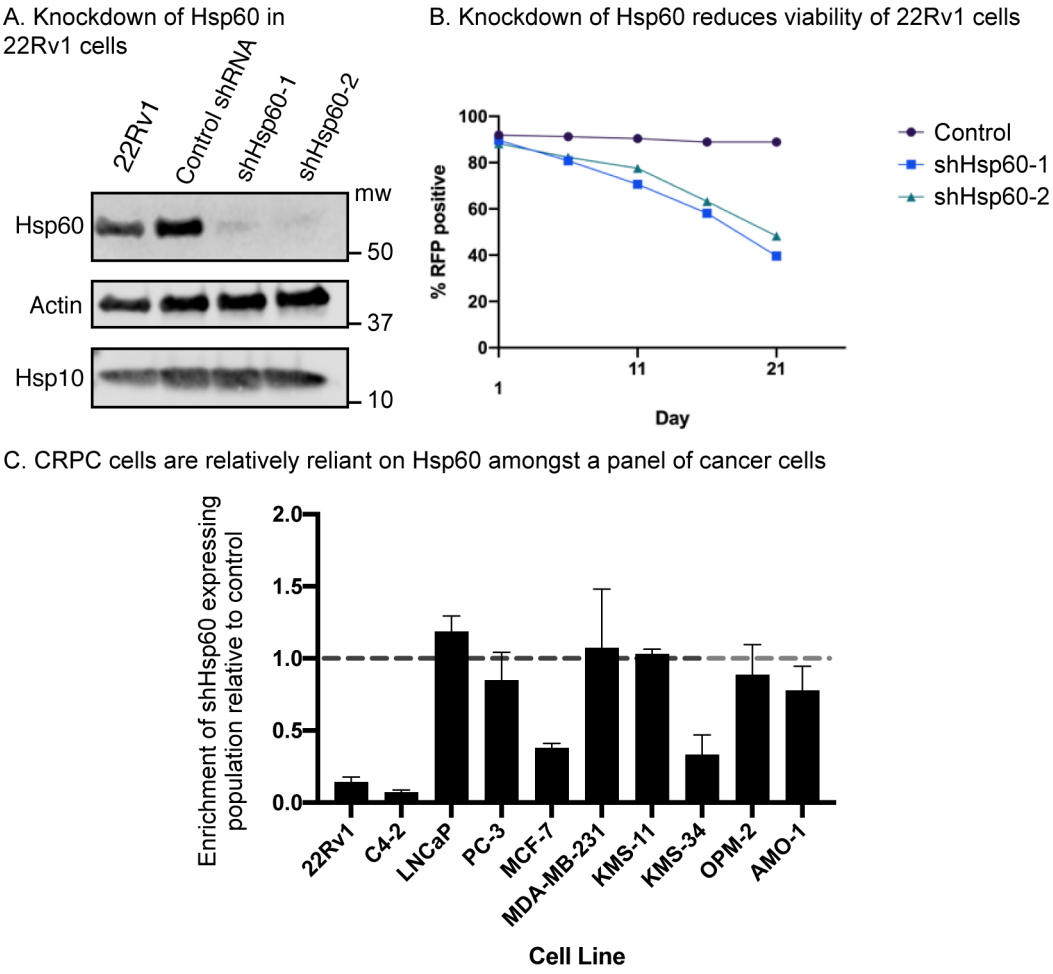

Figure 4.

Validation of Hsp60 as a selective vulnerability in CRPC cell lines. A. 22Rv1 cells were transduced with either a control or Hsp60 targeting shRNA, which induced robust knockdown (>90%). Results are representative of experiments performed in triplicate B. The shRNA expressing population was monitored via flow cytometry through RFP expression. Over time, the population of Hsp60 knockdown cells decreased compared to the control shRNA. C. A panel of additional cancer cells were transduced with the Hsp60 shRNAs and the RFP-expressing population was monitored over time (~2–3 weeks). Hsp60 knockdown was strongly depleted in CRPC cells (22Rv1 and C4–2), but not in the other tested PCa, breast, or multiple myeloma cells. Enrichment was calculated as the ratio of (RFP+)/(1-RFP+) between the initial and final time point, relative to a control shRNA. Results are the average of two independent experiments and the error bars represent SD.

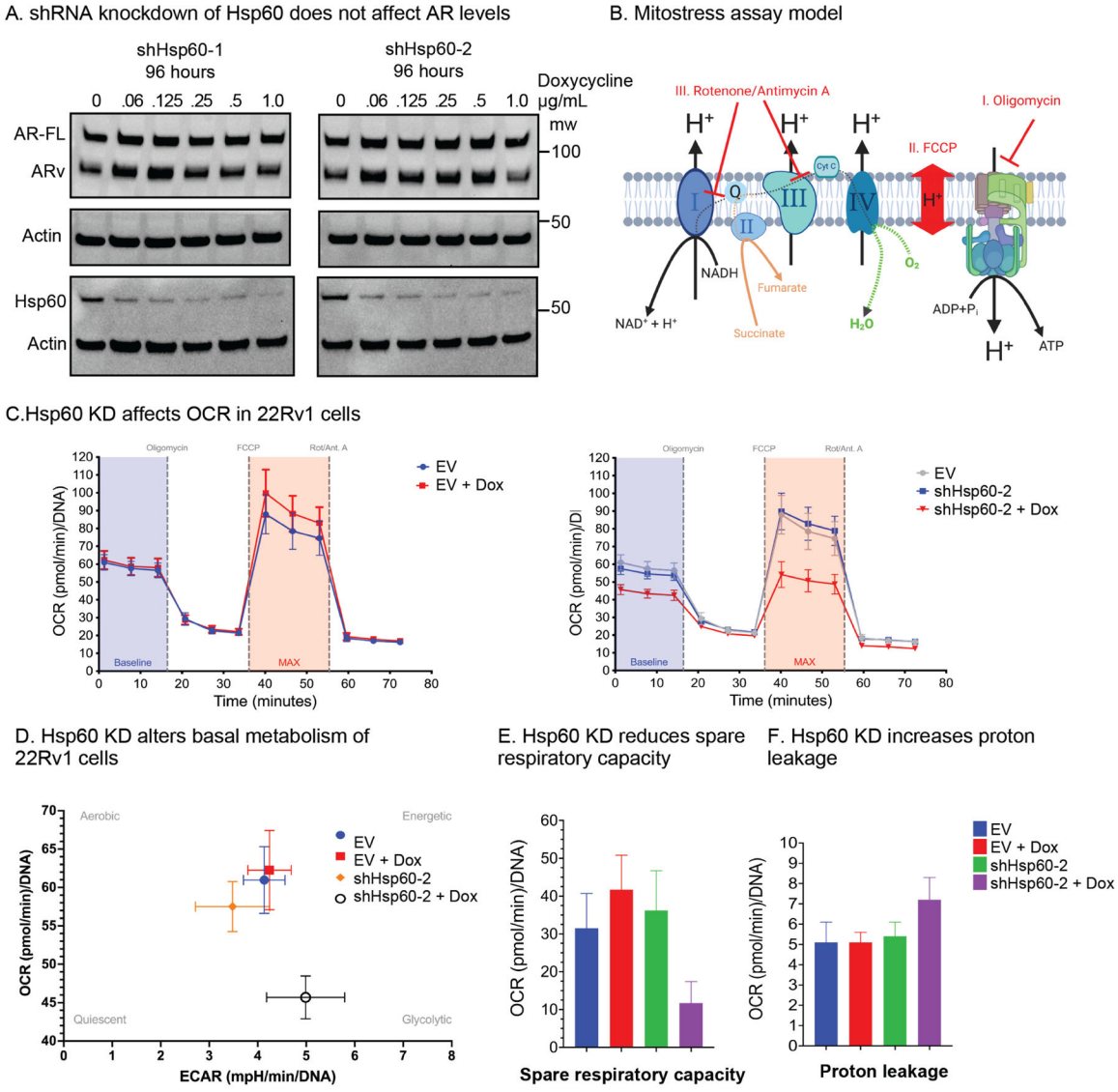

Figure 5.

Hsp60 knockdown does not affect AR but Hsp60 promotes mitochondrial respiration of 22Rv1 cells. A. Dox-inducible shRNAs of Hsp60 were stably expressed in 22Rv1 cells. shRNAs reduce Hsp60 levels, but both full-length and ARv levels are unaffected after 96 hr dox treatment. B. Model of mitostress assay overlayed on inner mitochondrial membrane and ETC. C. Mitostress analysis of 22Rv1 EV or dox-inducible shHsp60–2 +/− 5 day treatment with 100 ng/mL doxycycline. D. Energetic plot of basal metabolism of 22Rv1 EV or shHsp60–2 cells with and without doxycycline. E. Quantitation of spare respiratory capacity or F. proton leakage of 22Rv1 EV or Hsp60–3 +/− 5 day treatment with 100 ng/mL doxycycline. Results are the average of three technical replicates (n=3) and error bars represent SEM. In addition, the results are representative of an independent replicate (see Supplemental Figure 5B) and similar results were obtained with a second shRNA sequence (see Supplemental Figure 5A).

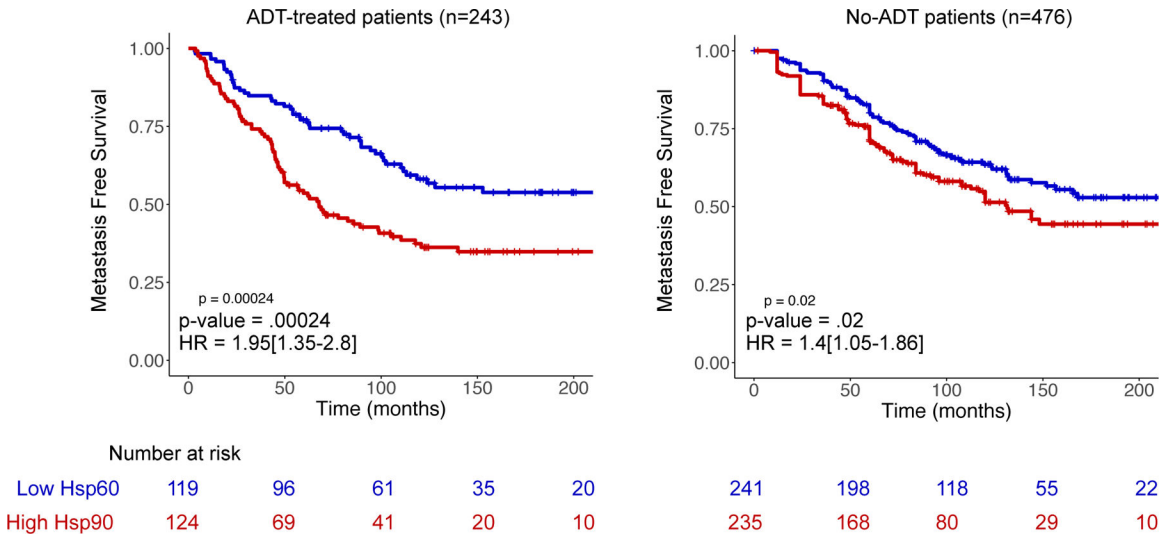

Figure 6:

Comparison of metastasis-free survival in patients with high (red, greater than median expression) or low (blue, lower than median expression) Hsp60 expression, with or without ADT treatment. Hsp60 expression significantly correlates with worse outcomes in ADT-treated prostate cancer patients. See the text for additional details.

KEY RESOURCES TABLE

REAGENT or RESOURCE	SOURCE	IDENTIFIER
Antibodies		
Anti-AR, rabbit monoclonal antibody	Abcam	Cat# ab133273
Anti-Hsc/p70, rabbit monoclonal antibody	San Cruz	Cat# sc33575
Anti-Hsp27, mouse monoclonal antibody	Santa Cruz	Cat# sc59562
Anti-Hsp60, rabbit monoclonal antibody	Cell Signaling	Cat# D6F1
Anti-Hsp10, mouse monoclonal antibody	Santa Cruz	Cat# sc376313
Anti-Actin, mouse monoclonal antibody	Sigma	Cat# A5441
Chemicals, peptides, and recombinant proteins		
JG-231	Shao et al. 2018	PMID: 29953808
AUY-922	Advanced ChemBlocks Inc.	Cat # 10274
bicinchoninic acid	ThermoFisher	Cat# 23227
polybrene	Santa Cruz	Cat# sc-134220
puromycin	Gibco	Cat# A11138–03
doxycycline	Millipore-Sigma	Cat# 1226003
protease inhibitors	Sigma	Cat# P8340
Lipofectamine 2000	Thermo Fisher	Cat# 11668019
penicillin-streptomycin	Millipore-Sigma	Cat# 11074440001
oligomycin,	Selleck Chem	Cat# S1478
trifluoromethoxy carbonylcyanide phenylhydrazone (FCCP)	Cayman	Cat#15218
rotenone/antimycin A	Sigma	Cat# R8875
non heat-inactivated fetal bovine serum	Gibco	Cat# 16000044
Q5® High-Fidelity polymerase	New England BioLabs	Cat# M0492S
M-PER extraction buffer	Millipore-Sigma	Cat# GE28–9412-79
Critical commercial assays		
MN NucleoSpin® Blood Kit	Macherey-Nagel	Cat# 740951
Cyquant	Thermo-Fisher	Cat# C35011
MTT assay	Sigma	Cat# 11465007001
Deposited data		
Decipher GRID database	Karnes et al. 2018	PMID: **29760221**
shRNA screening and data analysis (misc)	Kampmann et al. 2014	PMID: 24992097
Experimental models: Cell lines		
Human PC-3 cell line	ATCC	CRL-1435
Human LNCaP cell line	ATCC	CRL-1740
Human C4–2 cell line	ATCC	CRL-3314
Human 22Rv1 cell line	ATCC	CRL-2505
HEK293T cell line	ATCC	CRL-3216

REAGENT or RESOURCE	SOURCE	IDENTIFIER
Oligonucleotides		
Proteostasis shRNA Library	This work	Supplemental Table 1
Recombinant DNA		
dox-inducible vector, pMK1201	Kampmann et al. 2015	PMID: 26080438
packaging plasmid (pMol)	Kampmann et al. 2014	PMID: 24992097
packaging plasmid (pRSV)	Kampmann et al. 2014	PMID: 24992097
packaging plasmid (pVSV-g)	Kampmann et al. 2014	PMID: 24992097
lentiviral backbone vector, pMK1275	Kampmann et al. 2015	PMID: 26080438
Software and algorithms		
PRISM	Graphpad	https//www.graphpad.com
Wave	Agilent	https://www.agilent.com
Cluster	Eisen et al., 1998	http://bonsai.hgc.jp/~mdehoon/software/cluster/software.htm
Java TreeView	Saldanha, 2004	http://jtreeview.sourceforge.net
ImageLab	Biorad	https://www.bio-rad.com
Python	Python	https://www.python.org
Bowtie	Bowtie	http://sourceforge.net/projects/bowtie-bio/files/bowtie/1.0.0/